Kinetics of the Liquid-Phase Hydrogenation of Benzene and Some Monosubstituted Alkylbenzenes over a Nickel Catalyst

S. Toppinen,[†] T.-K. Rantakylä,[‡] T. Salmi,*[,†] and J. Aittamaa[§]

Laboratory of Industrial Chemistry, Åbo Akademi, FIN-20500 Åbo, Finland, Department of Process Engineering, University of Oulu, FIN-90570 Oulu, Finland, and Neste Engineering, P.O. Box 310, FIN-06101 Porvoo, Finland

The liquid-phase hydrogenation kinetics of benzene and three monosubstituted alkylbenzenes, toluene, ethylbenzene, and cumene, was determined in a semibatch reactor operating at hydrogen pressures of 20−40 atm and at temperatures of 95−125 °C. Commercial preactivated catalyst particles of nickel−alumina were used in all experiments. The hydrogenation activity of the compounds decreased in the order benzene ≫ toluene > ethylbenzene > cumene. The main reaction product was always the completely hydrogenated cycloalkane, whereas only trace amounts of cycloalkenes were detected. The hydrogenation rates had a slow initial period followed by a period of a virtually constant rate, which decreased at the end of the reaction. The analysis of the data with a reaction−diffusion model revealed that the kinetics was influenced by pore diffusion. Rate equations based on a sequential addition mechanism of adsorbed hydrogen to the aromatic nucleus were derived, and the kinetic parameters were estimated from the reaction−diffusion model with nonlinear regression analysis. The rate equations were able to describe all the features of the experimental data.

Introduction

The hydrogenation of aromatic hydrocarbons to the corresponding cyclic compounds,

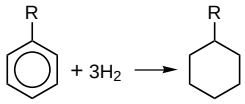

(1)

is of current interest in the industrialized world because of more strict environmental legislation. The total hydrogenation process (1) has for a long time been actual because of the production of some speciality chemicals, such as the synthesis of nylon, where cyclohexane is one of the key intermediates. Recent environmental awareness has, however, focused the attention on the hydrogenation for new reasons: the production of aromatic-free solvents—which is the current industrial reality—and the production of aromatic free traffic fuels—which represents the future. Thus, the trend of 1980s, when the addition of aromatic compounds in the gasoline was recommended as a way to increase the octane number, has been completely reversed in the 1990s: the aromatics are expected to be absent in the fuels of the 21st century.

Aromatic compounds are, however, present in the crude oil; a typical crude oil from the North Sea area (gasoline and middle distillate fractions) contains 10−20% of aromatic compounds. Furthermore, the future use of natural gas as a source of liquid fuel might utilize aromatization steps. For example, straight-chain hydrocarbons and methanol can be aromatized on zeolite catalysts.

Consequently, there is a need for the research of dearomatization. Traditionally the academic studies of hydrogenation of aromatics have concerned the gas-phase process, which can progress in the presence of several catalysts, such as Ni, Co, Pt, Pd, Ru, etc. (Bond, 1962). Numerous studies have been published on the gas-phase dearomatization; some previous works are described and summarized in detail in the references (Lindfors and Salmi, 1993; Lindfors *et al.*, 1993; Mirodatos, 1987). The studies of gas-phase hydrogenation serve for the understanding of the basic reaction mechanisms and the catalyst function. The large-scale processes in the refineries are, however, usually carried out in the liquid phase, in trickle bed reactors, where the feeds containing aromatics react with dissolved hydrogen on the surface of a catalyst. For the proper design of industrial dearomatization reactors, kinetic models for the reaction rates are invaluable.

The kinetics of the liquid-phase hydrogenation of aromatics has been considered, for example, by Murzin *et al.* (1989) and Temkin *et al.* (1989). The basic debate on the hydrogenation mechanism concerns the chemical state of the catalytically active hydrogen and the role of the reaction intermediates. Some authors propose that the active hydrogen might be in dissociated form on the catalyst surface, whereas others suggest that adsorbed molecular hydrogen might act as an active species in the hydrogenation. It is well-known that hydrogenation of benzene gives cyclohexene as a byproduct, particularly when the hydrogenation is carried out on Ru catalysts (Hartog *et al.*, 1961). Some cyclohexene has, however, been detected also in the hydrogenation of benzene on the commercial Ni catalyst. These experimental facts lead to the question of whether compounds like cyclohexadiene and cyclohexene are the real reaction intermediates or not. The overall hydrogenation kinetics can certainly be described with these intermediates, but there remains a doubt on the thermodynamic consistency of the rate models based on cyclohexenes and cyclohexadienes, since the hydrogenation rates of these compounds are known to be very high compared to the hydrogenation rate of the corresponding aromatic compound. However, rate equations, where the hydrogenation of compounds like C_6H_8 and C_6H_{10}

* Author to whom correspondence is addressed. Telephone: +358-21-2654427. Fax: +358-21-2654479. E-mail: Tapio.Salmi@abo.fi.
[†] Åbo Akademi.
[‡] University of Oulu.
[§] Neste Engineering.

S0888-5885(95)00431-3 CCC: $12.00

are rate-determining steps, describe well the experimental data obtained for gas-phase hydrogenation. This dilemma has been solved in some recent research by proposing that the kinetically plausible intermediates C_6H_8 and C_6H_{10} preserve an aromatic character (Temkin *et al.*, 1989; Smeds *et al.*, 1995), and they do not represent the corresponding hexenes and hexadienes.

The research of the liquid-phase hydrogenation has mainly concerned the hydrogenation of benzene as a model substance. The feed to a typical dearomatization unit contains, however, a lot of C_7-C_{12} hydrocarbons, i.e., different kinds of substituted alkylbenzenes. Consequently, the endeavor of the present work is to determine the liquid-phase hydrogenation kinetics of benzene and some monosubstituted benzenes, in order to reveal the role of the alkyl chain on the reactivities of the substituted benzenes.

Experimental Section

The kinetic experiments were carried out in a computer controlled reactor system manufactured by Xytel B. V. Europe. The reactor was controlled by an integrated control system, which was run under a PC-DOS microcomputer. The PC computerized all the main control and monitoring actions, providing also data acquisition and scheduling facilities. The reactor (inner diameter 100 mm, total volume 1000 mL) was operated in a semibatch mode in which hydrogen was fed into the reactor to maintain the pressure constant during the experiments. The desired reactor pressure was adjusted by the supply pressure of hydrogen. Hydrogen flow rates were controlled and measured by using a mass flowmeter (Bronkhorst High-Tech F 231C-FA). The reactor was equipped with a magnetic propeller stirrer, whose speed motor was installed with computer monitoring and set point adjusting. The reactor was heated in a three-zone electric-heat furnace, and the temperatures of the heating jackets were controlled by a computer. The reactor was equipped with two internal thermocouples. The catalyst was placed in a static basket.

The three-phase hydrogenation of aromatics was studied on a commercial nickel−alumina catalyst (Crosfield; Ni 16.6 wt %, specific surface area 108 m^2/g, mean pore volume 0.37 cm^3/g, bulk density 0.86 g/cm^3). Hydrogen was supplied by AGA (>99.9995%). The model compounds used in these experiments were as follows: benzene (>99.7%, Merck), toluene (>99%, J.T. Baker), ethylbenzene (>98%, Fluka), and cumene (>98%, Fluka).

Samples were analyzed by a gas chromatograph (Hewlett-Packard 5830A) equipped with a 30 m long capillary column (J&W Scientific, DB-624) and a flame-ionization detector (FID). The column temperature was 100 °C in experiments with toluene, ethylbenzene, and cumene and 60 °C in those with benzene. The identification of hydrogenated products was done by using gas chromatograph−mass spectrometer (GC−MS) analysis.

Kinetic experiments were carried out at pressures of 20 and 40 bar and at temperatures of 95 and 125 °C. In addition to this, the hydrogenation of toluene was also investigated at 10 and 30 bar and at 140 °C. The amount of catalyst was 10 g in the experiments performed at 125 °C, and it was increased to 30 g when operated at the lowest temperature. The particle size of catalyst extrudate used in these experiments was as follows: mean particle length of 3 mm and mean particle diameter of 1 mm.

The activation of the nickel catalyst was performed before each experiment in order to keep the catalyst activity at a constant level. The activation treatment was done at atmospheric pressure by flowing hydrogen (3 dm^3/min). During the activation, first, the catalyst was heated to 120 °C and maintained at that stage for 1 h, and, second, the temperature was increased to 260 °C at a rate of 80 °C /h. The hydrogen flow was continued at 260 °C for 1.5 h. Then, the reactor was cooled down to 80 °C under a small hydrogen flow (0.2 dm^3/min). The activation procedure was carried out automatically using recipe and scheduling programs available in the control system package. Therefore, the possible differences between activation treatments were eliminated.

Typically the pure aromatic reagent (335 mL) was loaded into the reactor through the feeding tube by using hydrostatic pressure of the liquid. Based on preliminary tests, a stirrer speed of 1900 rpm was chosen to be suitable for the elimination of external mass-transfer resistances. Temperature and pressure values were adjusted to desired values and after 20 min the first sample was taken for GC analysis. Sampling intervals were approximately 30 min, except when the aromatic concentration was lower than 15%, more frequent intervals were used (10−15 min).

The duration of experiments varied from 2 to 7 h depending on conditions and amounts of the catalyst.

The temperature was controlled within ±4 °C of the desired value and the pressure varied within ±0.3 bar, but at the end of experiment, when aromatic concentration was low, pressure increased about 10% from the desired value. After the experiment the reactor was emptied and rinsed using nitrogen flow and heat treatment.

Results and Discussion

Qualitative Considerations. The results revealed that the main hydrogenated products of benzene, toluene, ethylbenzene and cumene were cyclohexane, methylcyclohexane, ethylcyclohexane, and isopropylcyclohexane, respectively. Small traces of other compounds were detected, but the identification was uncertain because of the extremely small amounts (totally < 0.5 wt %) of observed compounds. Thus, the trace components can be discarded in modeling of the hydrogenation kinetics.

The measured concentration trends in the hydrogenation experiments are illustrated in Figures 1a−d using $t' = tm_{cat}/V_L$ as the abscissa. In that way the experiments with different amounts of catalyst and different liquid loadings can be directly compared. If the evaporation of the liquid into the gas phase is neglected, the mass balance of the liquid components is

$$dn_{Li}/dt = m_{cat}r_i \qquad (2)$$

where the generation rate (r_i) is given per catalyst mass (m_{cat}). If, furthermore, the volume of the liquid phase (V_L) is constant, eq 2 can be simplified to

$$dc_{Li}/dt' = r_i = \nu_i R \qquad (3)$$

i.e., the rates are proportional to the slopes of the curves in Figures 1a−d. The catalyst amount was 10 g in all the experiments at 125 °C and 20 g (with ethylbenzene and cumene) or 30 g (with benzene and toluene) in the experiments at 95 °C. The liquid volume varied between 325 and 335 mL.

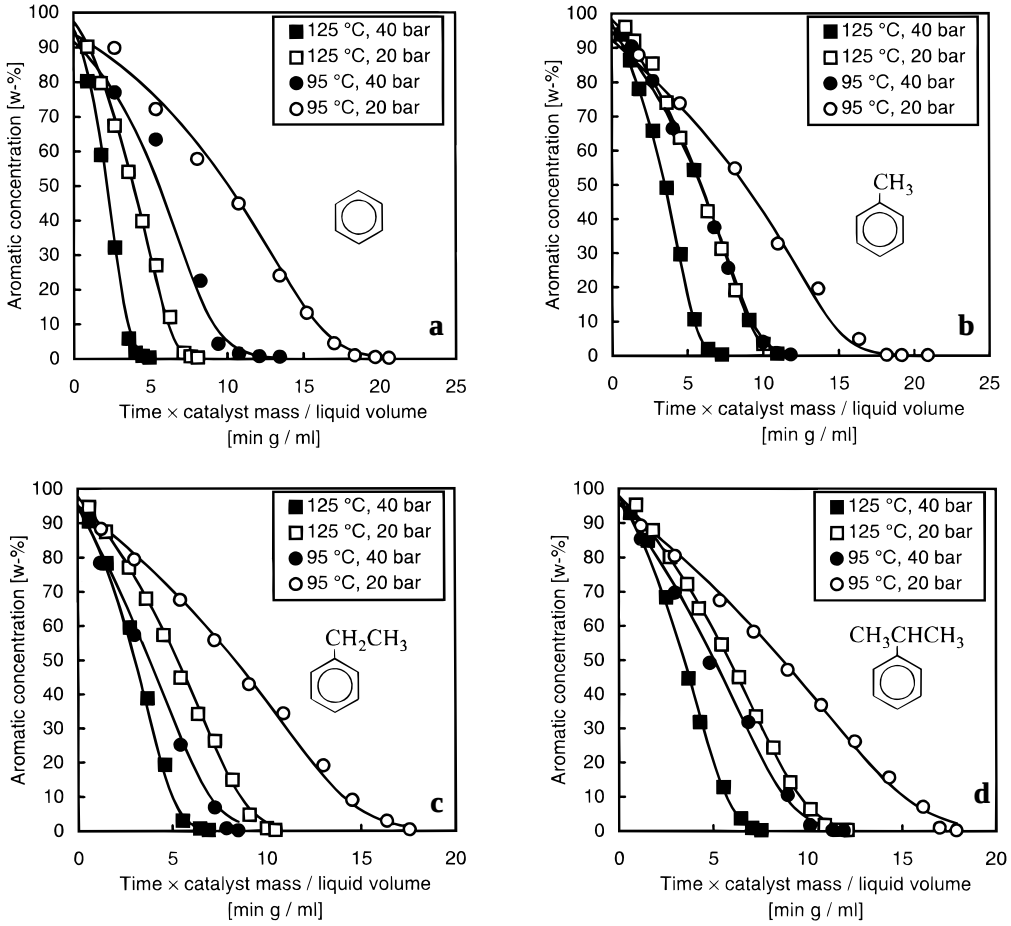

Figure 1. Measured (symbols) and estimated (curves) aromatic concentrations of benzene (a), toluene (b), ethylbenzene (c), and cumene (d) experiments. Mechanism I with dissociative adsorption of hydrogen.

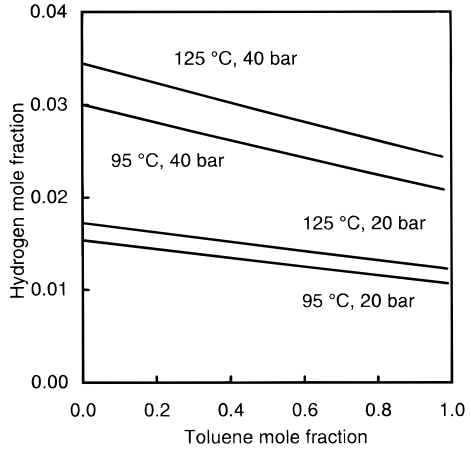

Figure 2. Solubility of hydrogen in the mixture of toluene and methylcyclohexane computed using the Soave−Redlich−Kwong equation of state.

The middle parts of the concentration curves are almost straight lines, suggesting that the reaction is nearly zero order with respect to the aromatic concentration. At very low aromatic concentrations the reaction seems to become first order. An interesting observation is that in the beginning of experiments, where the aromatic concentration has a maximum, the reaction rate is lower than in the middle of the experiments. This effect can be partly explained by the increasing solubility of hydrogen into the liquid mixture. Some solubility data are shown in Figure 2. In addition, in the very beginning of the experiments the temperature had not fully reached its desired value. However, in order to explain the negative reaction order with the low temperature, the apparent activation energy should be as high as 100 kJ/mol, whereas the apparent activation energy was estimated to 25 kJ/mol (Figures 3a,b). This implies that the low reaction rate in the beginning of the experiments is mainly caused by kinetic effects.

To compare the effects of the temperature and pressure on the reaction rate, average reaction rates were calculated using the concentration interval 10−80 wt %, and plotted against temperature (Figures 3a,b) and pressure (Figures 4a,b). The figures show clearly that benzene is the most reacting model compound and that the reaction rate decreases with an increasing size of the substituent in the benzene ring in all the conditions studied. The apparent reaction order with respect to the hydrogen concentration, which is proportional to the pressure, seems to be a little less than 1.

Modeling of the Hydrogenation Kinetics. In the quantitative modeling of the experimental results, two kinds of reaction mechanisms were considered. First, a mechanism where hydrogen and the aromatic compound are adsorbed competitively on the surface of the catalyst and hydrogen is added to the aromatic ring in three sequential surface reaction steps (Smeds *et al.*, 1995), and, second, a mechanism where reaction occurs via an intermediate surface complex (Temkin *et al.*, 1989).

Smeds *et al.* (1995) studied gas-phase hydrogenation of ethylbenzene and suggested a mechanism (model I) where aromatic and hydrogen molecules are adsorbed competitively on the vacant catalyst active sites. Hydrogen is added to aromatic molecules in three sequen-

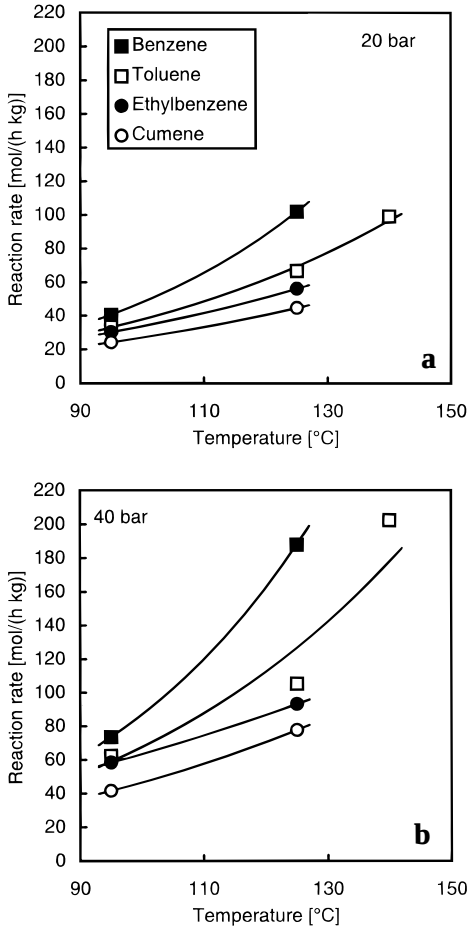

Figure 3. Average reaction rate as a function of reactor temperature at pressures 20 (a) and 40 bar (b).

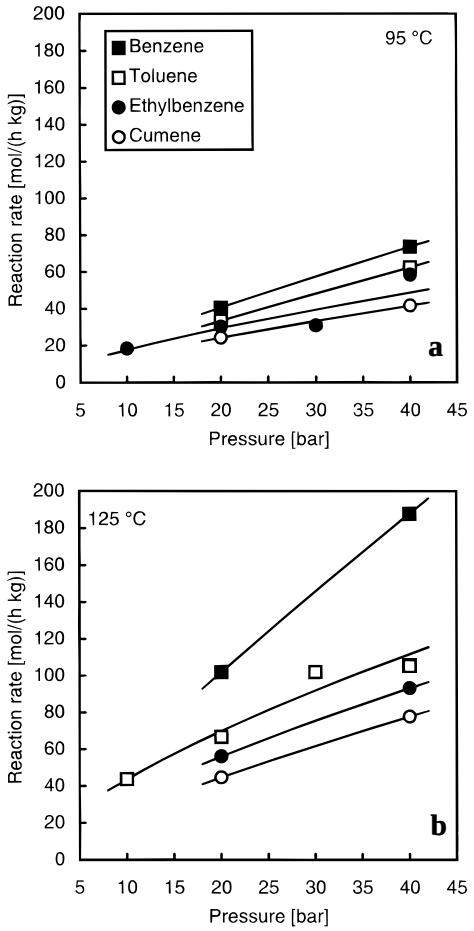

Figure 4. Average reaction rate as a function of reactor total pressure at temperatures 95 (a) and 125 °C (b).

tial surface reaction steps. For the sake of simplicity, it was assumed that both hydrogen and the hydrocarbons occupy just one active site. Preliminary tests showed that the assumption of aromatic adsorption on multiple sites did not improve the fit of the model. The mechanism can be described with the following reaction steps:

$$A^* + \gamma H_{2/\gamma}{}^* \underset{k_{-1}}{\overset{k_1}{\Leftrightarrow}} AH_2{}^* + \gamma^* \quad (4)$$

$$AH_2{}^* + \gamma H_{2/\gamma}{}^* \underset{k_{-2}}{\overset{k_2}{\Leftrightarrow}} AH_4{}^* + \gamma^* \quad (5)$$

$$AH_4{}^* + \gamma H_{2/\gamma}{}^* \underset{k_{-3}}{\overset{k_3}{\Leftrightarrow}} AH_6{}^* + \gamma^* \quad (6)$$

$$A + * \overset{K_A}{\Leftrightarrow} A^* \quad (7)$$

$$H_2 + \gamma^* \overset{k_H}{\Leftrightarrow} \gamma H_{2/\gamma}{}^* \quad (8)$$

$$AH_6{}^* + \xrightarrow{\text{rapid}} AH_6 + {}^* \quad (9)$$

where the hydrogen addition steps are assumed to be rate determining, and $\gamma = 1$ for nondissociative adsorption and $\gamma = 2$ for dissociative adsorption of hydrogen. The surface intermediates $AH_2{}^*$ and $AH_4{}^*$ are supposed not to be the substituted cyclohexadiene and cyclohexene but intermediates which preserve their aromatic character (Smeds *et al.*, 1995). Cyclohexadiene and cyclohexene are improbable intermediates since the hydrogenation rates of these compounds are known to be very high.

In the derivation of the rate equation we assume that the surface reactions are rate determining, whereas the adsorption steps of hydrogen and the aromatic compound are rapid enough for the quasi-equilibrium hypothesis to be applied. The quasi-equilibrium approximation of the adsorption steps gives

$$K_A = \frac{\Theta_A}{c_A \Theta_v} \quad (10)$$

$$K_H = \frac{\Theta_H^\gamma}{c_{H_2} \Theta_v^\gamma} \quad (11)$$

where Θ_v is the fraction of the vacant sites on the catalyst surface. The stationary state assumption for the adsorbed surface intermediates AH_2* and AH_4* gives

$$r_{AH_2{}^*} = k_1 \Theta_A \Theta_H^\gamma - k_{-1} \Theta_{AH_2} \Theta_v^\gamma - k_2 \Theta_{AH_2} \Theta_H^\gamma + k_{-2} \Theta_{AH_4} \Theta_v^\gamma = 0 \quad (12)$$

$$r_{AH_4{}^*} = k_2 \Theta_{AH_2} \Theta_H^\gamma - k_{-2} \Theta_{AH_4} \Theta_v^\gamma - k_3 \Theta_{AH_4} \Theta_H^\gamma + k_{-3} \Theta_{AH_6} \Theta_v^\gamma = 0 \quad (13)$$

By solving eqs 10−13 and the site balance:

$$\Theta_A + \Theta_{AH_2} + \Theta_{AH_4} + \Theta_{AH_6} + \Theta_H + \Theta_v = 1 \quad (14)$$

the fractional surface coverages can be obtained ($\Theta_{AH_6} = 0$ due to rapid desorption of cyclohexane). The equations for the fractional coverages are given in the appendix. The rate of the overall reaction (1) is then obtained by substituting the fractional coverages into the rate expression:

$$R = k_1\Theta_A\Theta_H^{\gamma} - k_{-1}\Theta_{AH_2}\Theta_v^{\gamma} = \frac{k_1k_2k_3K_AK_H{}^3c_Ac_{H_2}{}^3}{\alpha\left[\frac{\beta}{\alpha}K_Ac_A + (K_Hc_{H_2})^{1/\gamma} + 1\right]^{\gamma+1}} \quad (15)$$

where

$$\alpha = k_2k_3K_H{}^2c_H{}^2 + k_3k_{-1}K_Hc_H + k_{-1}k_{-2} \quad (16)$$

$$\beta = (k_1k_2 + k_1k_3 + k_2k_3)K_H{}^2c_H{}^2 + (k_1k_{-2} + k_3k_{-1})K_Hc_H + k_{-1}k_{-2} \quad (17)$$

Temkin *et al.* (1989) have proposed a mechanism (model II), where the aromatic molecule, e.g., benzene, forms an intermediate complex with hydrogen. The complex is then isomerized to adsorbed cyclohexene and rapidly hydrogenated to cyclohexane. The aromatic molecules are adsorbed on the catalyst surface by replacing adsorbed cyclohexane molecules. The mechanism can be described with the following reaction steps:

$$A^* + H_2 \underset{k_{-1}}{\overset{k_1}{\rightleftharpoons}} A(H_2)^* \quad (18)$$

$$A(H_2)^* + H_2 \underset{k_{-2}}{\overset{k_2}{\rightleftharpoons}} A(H_2)_2{}^* \quad (19)$$

$$A(H_2)_2{}^* \xrightarrow{k_3} AH_4{}^* \quad (20)$$

$$AH_4{}^* + H_2 \xrightarrow{\text{rapid}} AH_6{}^* \quad (21)$$

$$A + AH_6{}^* \overset{K_4}{\rightleftharpoons} A^* + AH_6 \quad (22)$$

By making the stationary state assumption for the surface components and by assuming the quasi-equilibrium of the desorption step (eq 22), the fractional coverages can be obtained (see appendix). The rate of the overall reaction becomes

$$R = k_3\left[1 + \frac{k_{-2} + k_3}{k_2c_H} + \frac{k_{-1}k_{-2} + k_{-1}k_3 + k_2k_3c_H}{k_1k_2c_H^2}\left(1 + \frac{c_{AH_6}}{K_4c_A}\right)\right]^{-1} \quad (23)$$

The experiments with one model compound were made only in two different temperatures and pressures, and the data therefore contain fairly little information on the temperature and pressure dependence of the reaction rate. The presented rate expressions (eqs 15 and 23) need thus to be simplified for the parameter estimation.

The rate expression of model I was simplified by assuming that the hydrogenation steps are irreversible

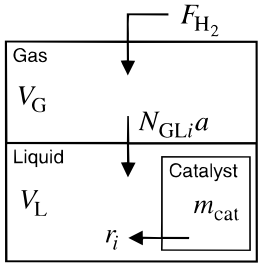

Figure 5. Mass transfer and reaction in the reactor model.

($k_{-1} = k_{-2} = k_{-3} = 0$) and have equal rate constants ($k_1 = k_2 = k_3$):

$$R = \frac{k_1K_AK_Hc_Ac_H}{[3K_Ac_A + (K_Hc_H)^{1/\gamma} + 1]^{\gamma+1}} \quad (24)$$

The temperature dependence of the adsorption coefficients K_A and K_H were assumed to be negligible, and the rate constant k_1 was assumed to depend on the temperature according to Arrhenius' law:

$$k_1 = k_1(T_0)\exp\left[-\frac{E_a}{R}\left(\frac{1}{T} - \frac{1}{T_0}\right)\right] \quad (25)$$

where a temperature of 100 °C was used as the reference temperature T_0.

The rate expression of model II was simplified by assuming the first two reaction steps (eqs 18 and 19) to be irreversible ($k_{-1} = k_{-2} = 0$) and the second reaction to be rapid compared to the first reaction ($k_1 \ll k_2$). The simplified rate expression is thus

$$R = \frac{k_1c_Ac_H}{\frac{k_1}{k_3}c_Ac_H + \frac{1}{K_4}c_{AH_6} + c_A} \quad (26)$$

The adsorption equilibrium coefficient K_4 was assumed to be independent of temperature, and Arrhenius' law was used for the rate constants k_1 and k_3.

A dynamic model was written for the laboratory reactor. Since the reactor temperature was measured during the experiments, the energy balances were not needed. The gas and the liquid phases in the reactor were assumed to be completely backmixed. The mass balances of the liquid and the gas phases are thus (Figure 5)

$$dn_{Li}/dt = V_RN_{GLi}a + m_{cat}r_i \quad (27)$$

$$dn_{Gi}/dt = -V_RN_{GLi}a + F_i \quad (28)$$

where V_R is the reactor volume and $N_{GLi}a$ denotes the volumetric mass-transfer flux of component i from the gas phase to the liquid phase. Equation 27 implies that the mass- and heat-transfer resistances around the catalyst particles and inside the particles were ignored.

The hydrogen feed to the reactor was obtained by simulating a P-controller:

$$F_{H_2} = K_p(V_R - V_L - V_G), \qquad F_i = 0, \quad i \neq H_2 \quad (29)$$

where the volumes of the liquid and gas phases (V_L and V_G, respectively) were calculated using the measured reactor pressure and temperature. The mass-transfer fluxes between the liquid and gas phases were obtained

Table 1. Estimated Parameters of the Rate Expression (24): Model I with Dissociative Adsorption of Hydrogen ($\gamma = 2$)

parameter	benzene	toluene	ethylbenzene	cumene
$k_1(T_0)$, mol/(s kg)	1.7 ± 0.8[a]	3.0 ± 1.0	5.7 ± 3.4	7.2 ± 3.7
E_a, kJ/mol	37.7 ± 1.9	16.8 ± 0.9	18.2 ± 1.6	15.6 ± 1.0
$K_A \times 10^5$, m^3/mol	11.9 ± 4.1	11.9 ± 1.8	9.8 ± 1.5	8.9 ± 0.9
$K_H \times 10^4$, m^3/mol	74.3 ± 69.1	21.9 ± 11.4	7.2 ± 5.5	4.2 ± 2.6
RRMS[2]	3.12	1.92	2.22	1.68
RSS	292	132	158	107
total RSS	689			

[a] 95% confident intervals. [b] Residual root mean square.

Table 2. Estimated Parameters of the Rate Expression (24): Model I with Molecular Adsorption of Hydrogen ($\gamma = 1$)

parameter	benzene	toluene	ethylbenzene	cumene
$k_1(T_0)$, mol/(s kg)	0.41 ± 0.10	0.46 ± 0.08	0.66 ± 0.19	0.66 ± 0.16
E_a, kJ/mol	37.6 ± 2.0	16.9 ± 1.0	18.2 ± 1.4	15.7 ± 1.0
$K_A \times 10^4$, m^3/mol	3.3 ± 2.0	3.6 ± 1.2	2.3 ± 0.5	2.0 ± 0.3
$K_H \times 10^3$, m^3/mol	10.6 ± 7.4	6.7 ± 2.8	2.9 ± 1.2	2.2 ± 0.7
RRMS	3.23	2.22	2.07	1.59
RSS	314	178	137	96
total RSS	725			

using the two-film theory:

$$N_{GLi}a = \frac{\frac{c_{Gi}}{K_i'} - c_{Li}}{\frac{1}{k_{Gi}aK_i'} + \frac{1}{k_{Li}a}} \tag{30}$$

where $k_{Li}a$ and $k_{Gi}a$ denote the volumetric mass-transfer coefficients of the liquid and the gas films, respectively, and the modified vaporization equilibrium constants are

$$K_i' = K_i\frac{c_{Gtot}}{c_{Ltot}} \tag{31}$$

The vaporization equilibrium constants (K_i) were obtained using the Soave−Redlich−Kwong equation of state (Graboski and Daubert, 1978). In this work the gas−liquid mass-transfer resistance was eliminated in the experiments using vigorous stirring. In the reactor simulation the effect of external mass-transfer limitations was therefore eliminated by using big values for the mass-transfer coefficients ($k_{Li}a = 10^2$ 1/s, $k_{Gi}a = 10^4$ 1/s).

The reactor model, the system of ordinary differential equations (ODE) (eqs 27 and 28), was solved numerically using the backward difference method (FORTRAN subroutine LSODE; Hindmarsh, 1983).

The parameter estimation of the kinetic parameters was performed with an adaptive nonlinear least-squares algorithm NL2SOL (Dennis *et al.*, 1981), which minimized the residual sum of squares (RSS) between the experimental and estimated aromatic contents (in weight percent). The first analysis (at $t = 0$ min in Figure 1a−d) was used as the initial state for the reactor simulation, and all the remaining observations were included in the RSS. The mass fractions in the liquid phase were calculated from the liquid mole fractions as:

$$w_i = x_iM_i/\sum_i x_iM_i \tag{32}$$

where M_i is the molar mass of the compound i.

For model I (eq 24) the kinetic parameters were estimated by assuming both the dissociative adsorption (Table 1) and the nondissociative adsorption (Table 2) of hydrogen. The estimated concentration curves were very similar in both cases. The model with dissociative adsorption of hydrogen gave a better fit with benzene and toluene data but a worse fit with ethylbenzene and cumene data than the model with nondissociative adsorption.

The estimated adsorption coefficients of the aromatic compounds are approximately equal, whereas the estimated adsorption coefficients of hydrogen decrease from benzene to cumene. Benzene deviates from the other model components by having a much greater activation energy for hydrogenation.

More sophisticated modifications of model I, e.g., a model containing temperature dependent adsorption coefficients as well as reversible hydrogenation steps, did not improve the fit significantly. Only minor reduction was achieved in RSS, whereas the standard deviations of the parameters increased notably.

The fit with model II (eq 26) was not fully successful since the value of the adsorption coefficient (K_4) was unlimitedly drifted up. The huge value of K_4 suggests that the catalyst surface was totally covered with adsorbed aromatic molecules, and thereby the reaction is zero order with respect to the aromatic concentration (almost straight concentration curves in Figures 6a−d); i.e., the reaction rate becomes

$$R = \frac{k_1c_H}{\frac{k_1}{k_3}c_H + 1} \tag{33}$$

Because of the unidentified parameter K_4, the parameters were estimated using rate equation (33) (Table 3).

Model II cannot predict negative orders of reaction with respect to the aromatic concentration, and therefore it is incapable of describing the period of the slower reaction in the beginning of the experiments. Similar results would be achieved with model I if noncompetitive adsorption would be assumed. The rate expression would be in that case (Smeds *et al.*, 1995)

$$R = \frac{k_1k_2k_3K_AK_H{}^3c_Ac_{H_2}{}^3}{\alpha\left[\frac{\beta}{\alpha}K_Ac_A + 1\right][(K_Hc_{H_2})^{1/\gamma} + 1]^\gamma} \tag{34}$$

In order to examine the effect of the mass-transfer limitations in the catalyst particles on the observed kinetics, the internal concentration and temperature profiles were modeled. The mass balance inside the

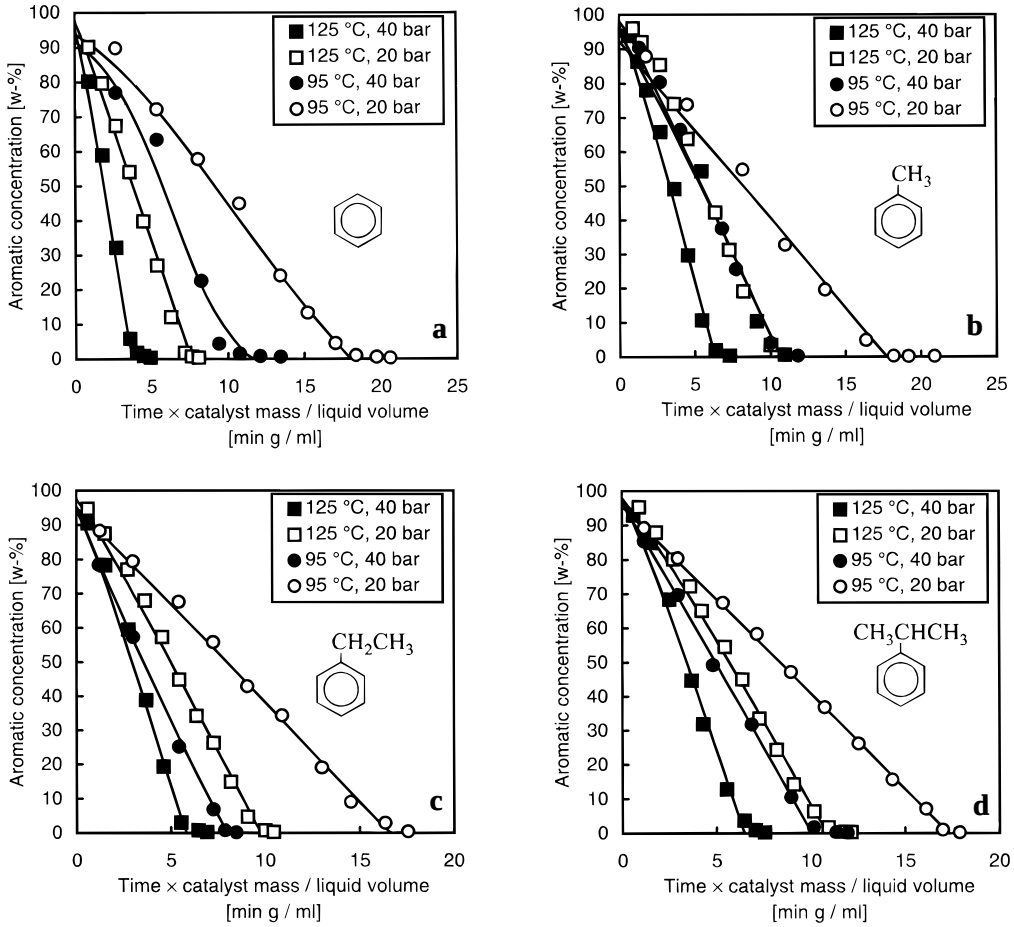

Figure 6. Measured (symbols) and estimated (curves) aromatic concentrations of benzene (a), toluene (b), ethylbenzene (c), and cumene (d) experiments. Mechanism II.

Table 3. Estimated Parameters of the Rate Expression (33): Model II

parameter	benzene	toluene	ethylbenzene	cumene
$k_1(T_0)$, mol/(s kg)	2.8 ± 1.1	1.3[a]	1.1 ± 0.1	1.0[a]
E_a, kJ/mol	1.6 ± 20.8	18.5[a]	25.2 ± 4.5	15.8[a]
$k_3(T_0)$, mol/(s kg)	3.4 ± 0.8	5.7[a]	10.1 ± 4.8	5.8[a]
E_a, kJ/mol	135.0 ± 46.9	11.5[a]	−13.0 ± 26.7	14.2[a]
RRMS	3.51	4.28	2.43	2.23
RSS	371	660	188	189
total RSS	1409			

[a] Confidence interval could not be estimated.

catalyst particle can be written for cylinder geometry:

$$\frac{\partial c_i}{\partial t} = \frac{D_{i,\mathrm{eff}}}{\epsilon R_\mathrm{p}^{\,2}}\left(\frac{\partial^2 c_i}{\partial x^2} + \frac{1}{x}\frac{\partial c_i}{\partial x}\right) + \frac{\varrho}{\epsilon} r_i' \tag{35}$$

where r_i' denotes the intrinsic generation rate of component i and x is the dimensionless radial coordinate in the particle. The energy balance for the particle is

$$\frac{\partial T}{\partial t} = \frac{\lambda}{\varrho c_\mathrm{p} R_\mathrm{p}^{\,2}}\left(\frac{\partial^2 T}{\partial x^2} + \frac{1}{x}\frac{\partial T}{\partial x}\right) + \frac{(-\Delta H_\mathrm{R})}{c_\mathrm{p}} r_i' \tag{36}$$

Since the external mass-transfer resistance around the catalyst particles was assumed to be negligible, the boundary conditions at the surface of the particle are

$$c_i|_{x=1} = c_{\mathrm{L}i} \tag{37}$$

$$T|_{x=1} = T_\mathrm{L} \tag{38}$$

In the center of the particle concentration and temperature gradients vanish due to symmetry:

$$\left.\frac{\partial c_i}{\partial x}\right|_{x=0} = 0 \tag{39}$$

$$\left.\frac{\partial T}{\partial x}\right|_{x=0} = 0 \tag{40}$$

The flux at the catalyst surface, i.e., the apparent reaction rate affecting the liquid bulk mass balance, is

$$r_i = \frac{2D_{i,\mathrm{eff}}}{\varrho R_\mathrm{p}^{\,2}}\left.\frac{\partial c_i}{\partial x}\right|_{x=1} \tag{41}$$

The effective diffusion coefficients were computed from molecular diffusion coefficients using average values (Satterfield, 1970) for the porosity ($\epsilon = 0.5$) and the tortuosity factor ($\tau = 4.0$):

$$D_{i,\mathrm{eff}} = \frac{\epsilon}{\tau} D_i \tag{42}$$

The molecular diffusion coefficients were obtained from the equation (Wilke, 1950; Reid *et al.*, 1987):

$$D_i = (1 - x_i)/\sum_{j \neq i}(x_j/D_{ij}^\circ) \tag{43}$$

where the diffusion coefficients at infinite dilution (D_{ij}°) were calculated using the Wilke−Chang (1955) equation (Reid *et al.*, 1987). The catalyst density (ρ) was assumed to be 1300 kg/m^3 and the thermal conductivity

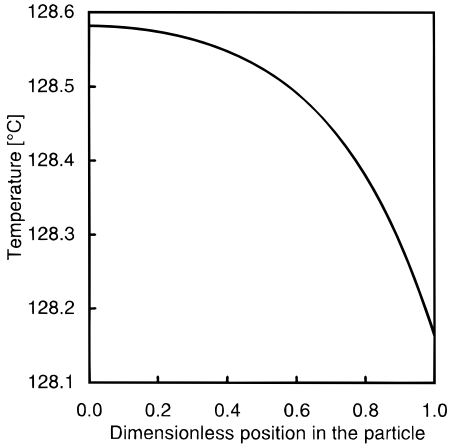

Figure 7. Temperature profile in the catalyst particles in the experiment with toluene at 40 bar and 125 °C.

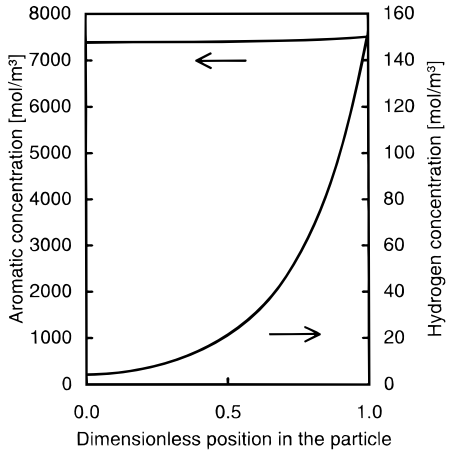

Figure 8. Concentration profiles in the catalyst particles in the experiment with toluene at 40 bar and 125 °C. Toluene concentration in the liquid phase was about 90 wt %.

(λ) 0.15 W $m^{-1}K^{-1}$. The particle radius (R_p) was 0.25 mm. A constant value of 210 kJ/mol was used for the reaction enthalpy ($-\Delta H_R$).

The radial concentration and temperature derivatives were discretized with central difference formulas, and the ODE system (eqs. 27, 28, 34, and 35) was solved using the backward difference method.

For diagnostic purposes the parameters of the rate expression (24) with dissociative adsorption of hydrogen were estimated using the data from toluene experiments and the heterogeneous reactor model. The simulation results showed convincingly that the heat-transfer limitation in the catalyst particles was negligible. The temperature in the center of the particles was at maximum 0.4 °C higher than the temperature of the liquid bulk (Figure 7). In contrast to that the effect of the mass-transfer was important. At higher aromatic concentrations (>5 wt %) the reaction rate was influenced by the hydrogen mass transfer (Figure 8). After the aromatic concentration decreased significantly, the mass transfer of the aromatic compound began to affect the reaction rate (Figure 9).

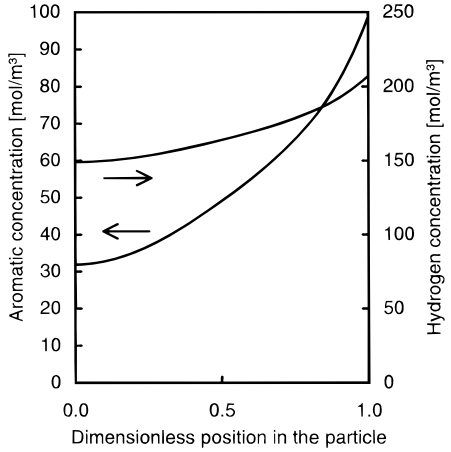

Figure 9. Concentration profiles in the catalyst particles in the experiment with toluene at 40 bar and 125 °C. Toluene concentration in the liquid phase was about 2 wt %.

The dynamic behavior of the profiles in the particle was examined by a separate simulation. At the initial state, zero concentration for hydrogen and the aromatic compound and an even temperature profile were assumed. The development of the profiles was simulated by assuming constant bulk phase concentrations and temperature. The simulation (Figures 10a−c) shows that the profiles reach their steady state in 20 s, which is a very short time compared to the time scale of the experiments.

In order to reduce the number of equations in the reactor model, the heat-transfer equations were neglected in the further treatment of the data. This was fully justified, since the heat-transfer limitation was negligible. The parameters of the best rate expression (24) were estimated for all model components (Table 4).

Conclusions

Hydrogenation experiments with benzene and three monosubstituted aromatics were carried out at two temperatures and two pressures. At all conditions studied, benzene appeared to be the most reactive aromatic compound and the hydrogenation rate was decreased with increasing length of the substituent in the benzene ring (Figures 3a,b and 4a,b). The highest reaction rate was achieved in the middle of the experiments (Figure 1a−d), not in the beginning, where the aromatic concentration was highest, suggesting negative order of reaction respect to the aromatic concentration in the beginning of the experiments.

Three mechanistic models were fitted to the experimental data. Model II proposed by Temkin *et al.* (1989)

Table 4. Estimated Parameters of the Rate Expression (24): Heterogeneous Reactor Model; Mechanism I with Dissociative Adsorption of Hydrogen (γ = 2)

parameter	benzene	toluene	ethylbenzene	cumene
$k_1(T_0)$, mol/(s kg)	1.3 ± 0.5	2.1 ± 0.7	5.2 ± 3.1	5.6 ± 2.7
E_a, kJ/mol	53.9 ± 2.9	20.0 ± 1.7	23.1 ± 2.3	19.0 ± 1.5
$K_A \times 10^4$, m^3/mol	18.3[a]	2.5 ± 1.1	1.3 ± 0.3	1.1 ± 0.2
$K_H \times 10^3$, m^3/mol	7074.5[a]	36.9[a]	3.9[a]	2.1 ± 1.4
RRMS	2.80	2.19	2.08	1.56
RSS	235	172	138	93
total RSS	639			

[a] Very large confidence interval.

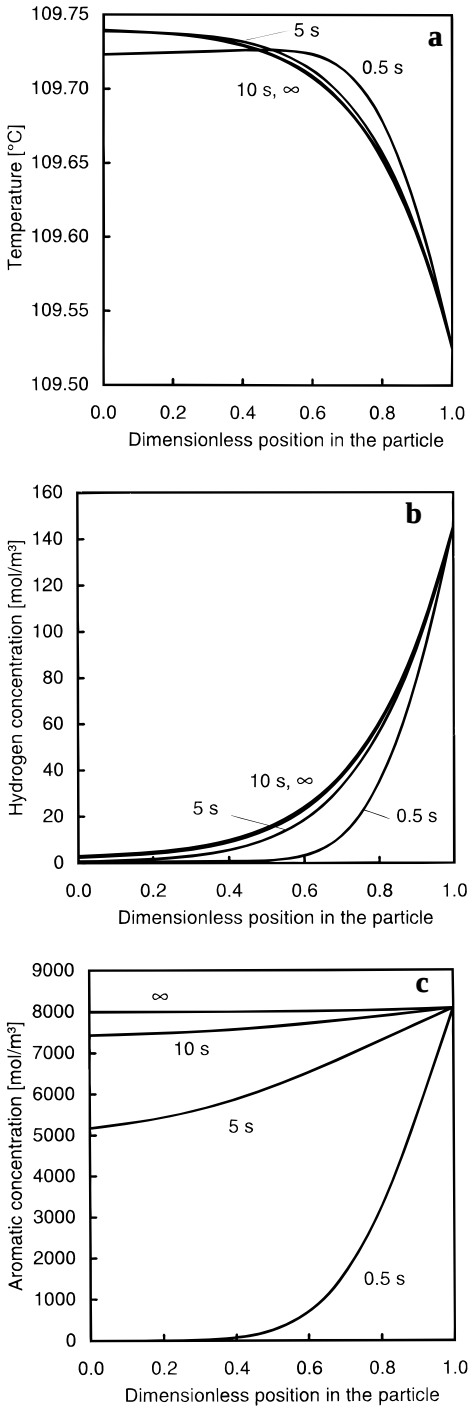

Figure 10. Development of temperature (a) and hydrogen (b) and aromatic (c) concentration profiles in the catalyst particle.

could not describe the slow reaction in the beginning of the experiments (Figures 6a−d), and it was therefore abandoned. Model I based on competitive adsorption of hydrogen and the aromatic compound fitted the data very well (Figure 1a−d). The model modifications with dissociative and nondissociative adsorption of hydrogen could not be discriminated based on the present data.

Simulations with a heterogeneous reactor model showed the hydrogenation reaction in the industrial-scale catalyst particles was significantly mass-transfer-controlled. The internal heat-transfer limitations were noticed to be negligible. Therefore, the kinetic parameters of model I we reestimated using the primary data and a priori estimated diffusion coefficients. The reestimation did not improve the overall fit of the model, but the model parameters became more realistic, because the mass transfer limitation was included in a theoretically correct way.

The present work concerned separate hydrogenation of aromatic compounds. In the future the research will be extended to mixtures of aromatic model molecules. The issues of crucial importance will become the competitive adsorption and the adsorptive interaction of the aromatics. The kinetic models presented here can, however, be easily generalized for multicomponent adsorption; e.g., additional adsorption steps analogous to eq 7 can be included in the model.

Acknowledgment

Financial support from Neste Oy Foundation is gratefully acknowledged.

Notation

a = gas−liquid mass-transfer area/reactor volume, m^{-1}
c_i = concentration of component i, mol m^{-3}
c_{Gi} = concentration of component i in the gas phase, mol m^{-3}
c_{Li} = concentration of component i in the liquid phase, mol m^{-3}
c_p = heat capacity of catalyst particles, kJ kg^{-1} K^{-1}
D_i = diffusion coefficient of component i, m^2 s^{-1}
$D_{i,eff}$ = effective diffusion coefficient of component i, m^2 s^{-1}
F_i = feed flow of component i to the reactor, mol s^{-1}
ΔH_R = reaction enthalpy, kJ mol^{-1}
k_{Gi} = gas-side mass-transfer coefficient of component i, m s^{-1}
k_{Li} = liquid-side mass-transfer coefficient of component i, m s^{-1}
K_i = vaporization equilibrium coefficient of component i
K_i' = modified vaporization equilibrium coefficient of component i
K_p = constant of the P-controller, mol s^{-1} m^{-3}
m_{cat} = catalyst mass, kg
n_{Gi} = molar amount of component i in the gas phase, mol
n_{Li} = molar amount of component i in the liquid phase, mol
N_{GLi} = gas−liquid mass-transfer flux of component i, mol m^{-2} s^{-1}
r_i = generation rate, mol s^{-1} kg^{-1}, $r_i = \nu_i R$
r_i' = intrinsic generation rate, mol s^{-1} kg^{-1}
R = reaction rate
R_p = radius of the catalyst particles, m
RRMS = residual root mean square
RSS = residual sum of squares
t = time, s
T = temperature, K
V_G = volume of the gas phase, m^3
V_L = volume of the liquid phase, m^3
V_R = reactor volume, m^3
x = dimensionless radial coordinate in the catalyst particles

Greek Letters

α = parameter in eq 15
β = parameter in eq 15
γ = number of active sites used for hydrogen molecule adsorption
ϵ = porosity of the catalyst particles
λ = thermal conductivity of catalyst particles, W m^{-1} K^{-1}
ν_i = stoichiometric coefficient
Θ_i = fractional coverage of component i

ρ = density of catalyst particles, kg m^{-3}
τ = tortuosity factor of the catalyst particles

Appendix

The fractional coverages with model I are

$$\Theta_v = \left[\frac{\beta}{\alpha}K_A c_A + (K_H c_{H_2})^{1/\gamma} + 1\right]^{-1} \quad \text{(A1)}$$

$$\Theta_H = (K_H c_{H_2})^{1/\gamma}\Theta_v \quad \text{(A2)}$$

$$\Theta_A = K_A c_A \Theta_v \quad \text{(A3)}$$

$$\Theta_{AH_2} = k_1(k_3 K_H c_{H_2} + k_{-2})K_A K_H c_A c_{H_2}\alpha^{-1}\Theta_v \quad \text{(A4)}$$

$$\Theta_{AH_4} = k_1 k_2 K_A K_H{}^2 c_A c_{H_2}{}^2\alpha^{-1}\Theta_v \quad \text{(A5)}$$

$$\Theta_{AH_6} = 0 \quad \text{(A6)}$$

The fractional coverages with model II are

$$\Theta_A = \left[k_1 k_2 c_{H_2}{}^2\varphi^{-1} + k_1(k_{-2} + k_3)c_{H_2}\varphi^{-1} + \frac{c_{AH_6}}{K_4 c_A} + 1\right]^{-1} \quad \text{(A7)}$$

$$\Theta_{A(H_2)} = k_1(k_{-2} + k_3)c_{H_2}\varphi^{-1}\Theta_A \quad \text{(A8)}$$

$$\Theta_{A(H_2)2} = k_1 k_2 c_{H_2}{}^2\varphi^{-1}\Theta_A \quad \text{(A9)}$$

$$\Theta_{AH_6} = \frac{c_{AH_6}}{K_4 c_A}\Theta_A \quad \text{(A10)}$$

where

$$\varphi = k_{-1}k_{-2} + k_{-1}k_3 + k_2 k_3 c_H \quad \text{(A11)}$$

Literature Cited

Bond, G. C. *Catalysis by Metals*; Academic Press Inc.: London, 1962; p 519.

Dennis, J. E.; Gay, D. M.; Welsch, R. E. An Adaptive Nonlinear Least-Squares Algorithm. *ACM Trans. Math. Software* **1981**, *7*, 369−383.

Graboski, M. S.; Daubert, T. E. A Modified Soave Equation of State for Phase Equilibrium Calculations. 1. Hydrocarbon Systems. *Ind. Eng. Chem. Process Des. Dev.* **1978**, *17*, 443−448.

Hartog, F.; Tebben, S. H.; Zwietering, P. *Actes Congr. Int. Catal., Ed. Technip.* **1961**, *1*, 1229.

Hindmarsh, A. C. ODEPACK, A Systematized Collection of ODE Solvers. In *Scientific Computing*; Stepleman, R. S., *et al.*, Eds.; . North-Holland: Amsterdam, The Netherlands, 1983; pp 55−64.

Lindfors, L. P.; Salmi, T. Kinetics of Toluene Hydrogenation on a Supported Nickel Catalyst. *Ind. Eng. Chem. Res.* **1993**, *32*, 34−42.

Lindfors, L. P.; Salmi, T.; Smeds, S. Kinetics of Toluene Hydrogenation on a Ni/Al_2O_3 Catalyst. *Chem. Eng. Sci.* **1993**, *48*, 3813−3828.

Mirodatos, C. Steady-State and Isotopic Transient Kinetics of Benzene Hydrogenation on Nickel Catalysts. *J. Catal.* **1987**, *105*, 405.

Murzin, D. Yu.; Solokova N. A.; Kul'kova, N. V.; Temkin, M. I. Kinetics of Liquid-Phase Hydrogenation of Benzene and Toluene on a Nickel Catalyst. *Kinet. Katal.* **1989**, *30*, 1352−1358.

Reid, R. C.; Prausnitz, J. M.; Poling, B. E. *The Properties of Gases and Liquids*; McGraw-Hill Book Co.: New York, 1987; p 741.

Satterfield, C. N. *Mass Transfer in Heterogeneous Catalysis*; MIT Press: Cambridge, MA, 1970; pp 38−39.

Smeds, S.; Murzin, D.; Salmi, T. Kinetics of Ethylbenzene Hydrogenation on Ni/Al_2O_3. *Appl. Catal. A* **1995**, *125*, 271−291.

Temkin, M. I.; Murzin, D. Yu.; Kul'kova, N. V. Mechanism of the Liquid-Phase Hydrogenation of the Benzene Ring. *Kinet. Katal.* **1989**, *30*, 637−643.

Wilke, C. R. Diffusional Properties of Multicomponent Gases. *Chem. Eng. Prog.* **1950**, *46*, 95−104.

Wilke, C. R.; Chang, P. Correlation of Diffusion Coefficients in Dilute Solutions. *AIChE J.* **1955**, *1*, 264−270.

Received for review July 12, 1995
Revised manuscript received December 29, 1995
Accepted January 23, 1996[⊗]

IE9504314

[⊗] Abstract published in *Advance ACS Abstracts*, April 1, 1996.